

# USING OF THE LOW TURBULENCE WIND TUNNEL FOR INVESTIGATION OF THREE-DIMENSIONAL UNSTEADY FLOW IN CURVED TUBES

Daniel Hanus, Pavel Anderle  
Czech Technical University in Prague, Czech Republic

**Keywords:** *Flows Mechanisms. Secondary Flows. Streamwise Vortices in Curved Channels*

## Abstract

*In the flow in curved channels (both stationary and rotating ones) which are used as basic working elements of turbomachines and jet engines important energy transformations proceed. The internal flow energy transformations in the curved tubes are accompanied by energy dissipation. The energy dissipation mechanism is in principle due to the friction forces caused by the viscosity and the turbulence of the flow with important transversal gradients of velocity within the channels. The energy loss is represented basically by the increase in entropy of the flow and demonstrated in general by loss of total pressure and by non-uniformity of the velocity and pressure fields. An important role in the total energy loss in the channels is played by the out-flowing vortex tubes generated in the flow by the action of the transverse pressure gradient arising as a result of centrifugal forces accompanying curved flow in the stationary channels or due to Coriolis forces in the case of rotating channels. A systematic experimental and theoretical investigation of the phenomena concerning the 3-D complex subsonic low speed flows within the channels, casings and curved tubes of jet engines and turbomachines were performed with special interest in the relationship between the value of the total losses and the geometry parameters of the curved channels. Further investigation of the relation between the flow structure and the turbulence at the inlet section of the curved tubes and the energy loss due to the circulation of the flow leaving the curved tubes has been carried out*

*using a specially designed open low turbulence wind tunnel.*

## 1 Nomenclature

$A$  = measuring plane at the inlet of the elbow  
 $B$  = measuring plane at the outlet of the elbow  
 $C$  = measuring plane at the exit from the pipe  
 $D$  = diameter of cross section of the tested elbow, mm

$$D_e = R_e \cdot \sqrt{\frac{D}{R}} \text{ Dean number}$$

$$M = \frac{w}{\sqrt{\kappa \cdot r \cdot T_s}} \text{ Mach number}$$

$p$  = pressure, Pa

$R$  = radius of the curvature of the center line of the elbow

$$R_e = \frac{w \cdot D}{\nu} \text{ Reynolds number}$$

$T$  = temperature

$w$  = velocity module  $\sqrt{(w_x^2 + w_y^2 + w_z^2)}$ , m/s

$Q$  = mass flow, kg/s

$\nu$  = kinematic viscosity, m<sup>2</sup>/s

$\rho$  = density, kg/m<sup>3</sup>

$\zeta$  = loss coefficient

$\omega$  = vorticity, s<sup>-1</sup>

## Subscripts

$d$  = dynamic

$kin$  = kinetic

$l$  = local (distribution)

$ref$  = upstream reference conditions

$s$  = static (pressure)

$t$  = total (pressure)

$tot$  = total (loss)

$u$  = transversal component (at the y-z plane)  
 $x$  = in the direction of the axis x  
 $y$  = in the direction of the axis y  
 $z$  = in the direction of the axis z

## 2 Introduction

In order to study, both experimentally and theoretically, flow mechanisms in curved channels, particularly with respect to the formation of the streamwise vortices [1] that contribute significantly to the well-known flow pattern of the secondary flows with a pair of counter-rotating vortex tubes, a simple experimental model of the curved tube was chosen. The tube is represented by an elbow of a circular cross-section with a bend of  $90^\circ$ . The biggest possible diameter of the tube was chosen to ensure detailed measurements within the channel by pneumatic and hot wire probes. The diameter of 300 mm is sufficiently large for this purpose and the energy requirements for creating the airflow of sufficient speed by the blower are met by the installed laboratory electrical supply. The chosen diameter allows further to test the channel with a naturally fully developed turbulent inlet flow modeled by a tube of a length of 60 diameters, that means the length of the pipe is 18 meters, which is the maximum allowed by the dimensions of the laboratory. The elbow consists of 7 segments as shown in Fig. 1.

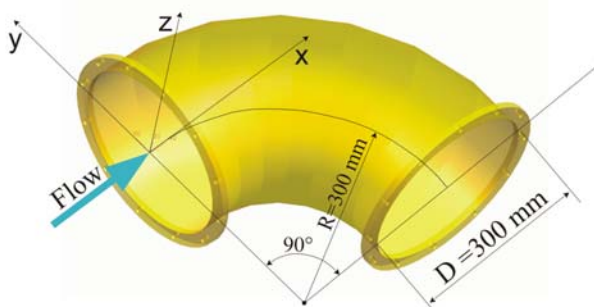


Fig.1. Segmented elbow

In order to study the influence of the geometrical shape of the elbow of the given Dean number, which is composed by the Reynolds Number and by the square root of the

ratio of the cross-section diameter of the elbow and the radius of the bend of its center line, a number of various experimental studies have been carried out with the turbulent flow at the inlet section of the elbow simulated by a short straight tube with a standardized measuring diaphragm [2]. The results of this investigation led to an improved design method of the inlet and outlet channels of jet engines. It was applied on the outlet channel of the two shaft Walter M601F turboprop engine of a max cruise power of 500 KW driving for example Let L 410 and Let L 420 light commuters. The new outlet channel with an energy loss of about one half of the original one provides the engine with another 18 kW of power without any rise in total fuel consumption. The same research led also to the design of a new inlet for the other, larger three-shaft Walter M 602 turboprop engine developed for the new L 610 commuter. Both newly designed and manufactured channels have met all airworthiness requirements and the inlet channel assured a very homogenous flow field in the inlet section of the first stage of the compressor.

Further investigations of the flow phenomena focus on the influence of the inlet flow field structure and its turbulence characteristics on the streamwise vortices generation and the losses caused by the accumulation of kinetic energy in the vortices screwing out continuously from the elbow.

The present introductory study is aimed at the evaluation of two different examples of inlet flow conditions for the same model of the elbow with the same value of the Mach number, Reynolds number and Dean number. The first case is characterized by a very uniform, laminar inlet flow with very low intensity of turbulence. This is attained by fitting the tested model close to the outlet section of the accelerating nozzle of the wind tunnel. The second case is considerably different from the first one. The inlet flow field is turbulent and the mean velocity distribution is given by the natural flow conditions for a complete development of a turbulent velocity profile in a circular pipe. This is attained by inserting, between the outlet flange of the accelerating nozzle of the wind

tunnel and the inlet flange of the tested model, a straight, smooth and sufficiently long pipe modeling the flow structure.

### 3 Tested model

As a tested model an arrangement of the described curved segmented channel and two short straight tubes has been chosen. The tested model consists of the assembly of the mentioned circular elbow and of the short pipe of the length of 300 mm in the front and of the longer pipe of the length of 1000 mm in the rear. The outlet section of the second pipe leads to the atmosphere. The design of the arrangement allows fit the measuring traversing apparatus to the flanges connecting the parts of the tested model in three principal positions. The first position at the inlet section of the elbow defines the measuring plane A. The second position at the outlet section of the elbow defines the measuring plane B. The third position at the outlet section of the tested model just before the flow leaves the tube for the atmosphere defines the measuring plane C. The measuring traversing apparatus is a semi-automatic device that is half manually and half computer operated to move and adjust the measuring probe in the measuring plane. A manually operated and adjustable rotating flange allows circumferential turns of the radial beam of the linear traversing bar holding the probe. The bar carries the rack that is displaced by the pinion driven

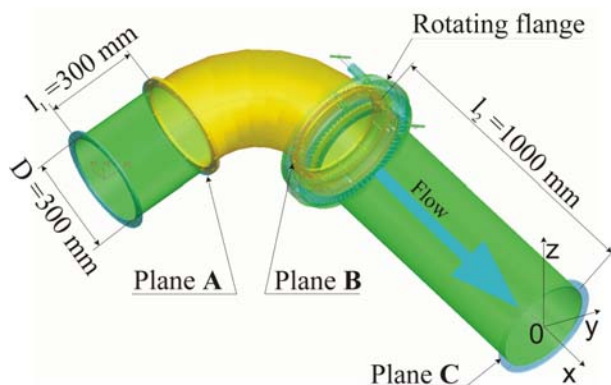


Fig. 2. Tested model

by an electric step motor controlled by the computer. The device is shown in Fig.3. The

elbow and both pipes carry static pressure probes on the walls.

### 4 Testing experimental device

To simulate the inflow conditions a new open type low turbulence wind tunnel has been designed using the CFD methods for the aerodynamic design [3] and overall design, manufactured and tested [4]. The tunnel is equipped with a very fine air filter allowing the use of thermo-anemometry methods for the measuring of the velocity fields in the unstationary and turbulent flows. The controlled and adjustable flow volumes of the air represented by the velocity at the outlet section of the accelerating nozzle are in the range from 10 to 60 meters per second. At the exit section of the nozzle the flow is laminar and rather homogenous with a very thin boundary layer of the thickness less than 1 mm. The measured streamwise component of intensity of turbulence at the exit section of the nozzle did not exceed 0.25%.

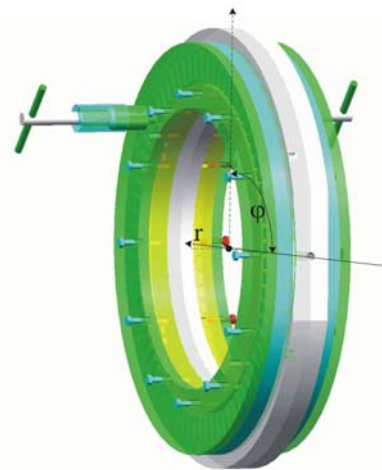


Fig. 3. Traversing device

The layout of the tunnel is shown in the Fig. 4.

The velocity distribution of the air at the outlet section of the accelerating nozzle is shown in Fig. 5.

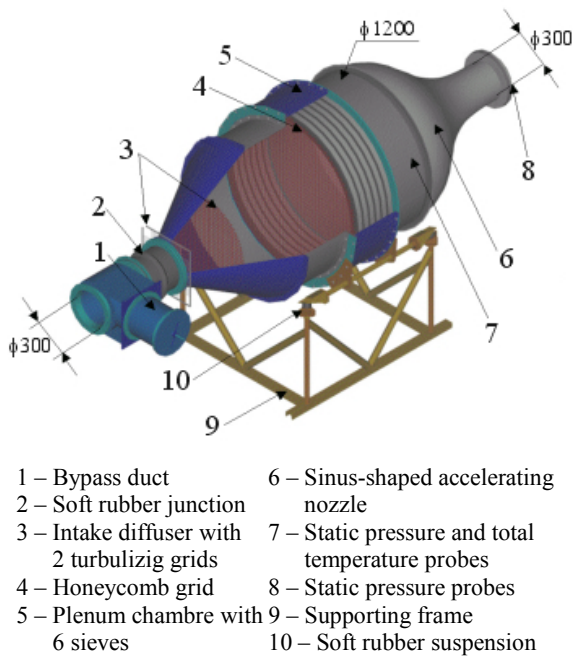


Fig. 4. Low turbulence wind tunnel

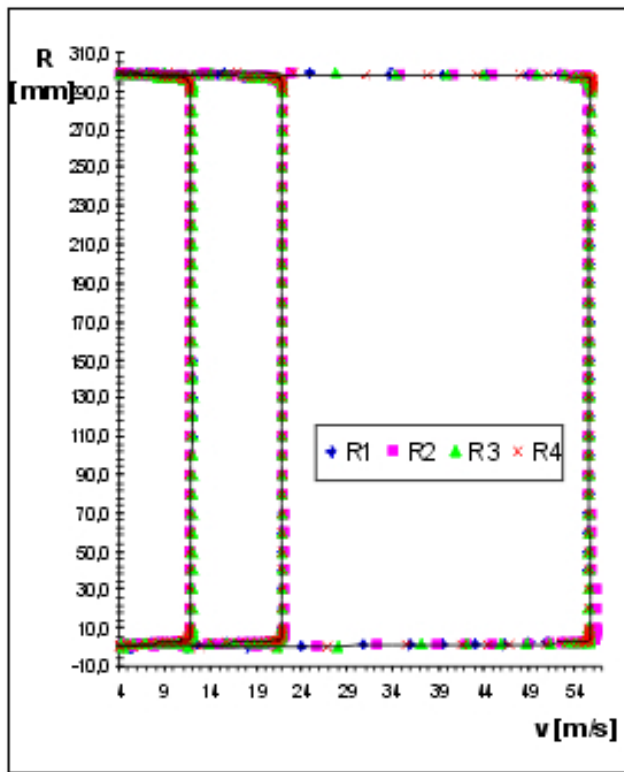


Fig. 5. Velocity distribution at the outlet section of the wind tunnel

### 5 Measuring method

As the first step of the evaluation of the 3-D flow fields the measuring of mean velocity within the tested model of a curved tube was chosen. For the measuring of the mean velocity vector field in the measuring plane a five-hole micro-probe with each sensor orifice outer diameter of 0.8 mm has been designed, manufactured and calibrated. A detailed picture of the probe is shown in Fig. 6. The measured five pressures are conducted by short tubes of a small diameter to a Pressure Systems Inc. pressure micro-scanner with a pneumatically controlled and computer operated switch and then transduced and converted to a digital signal and processed by computer. Together with the measured pressures of the probe the total temperature of the air is measured by a thermocouple placed inside the tube. The mass flow is detected by the pressure difference between static pressures measured in the plenum chamber of the wind tunnel and at the exit section of the accelerating nozzle.

The acquisition and sampling of the measured data is made by the National Instruments Data Acquisition System consisting of the AT-MIO-1 measuring card and the Lab View software. The system operates the traversing device in radial direction automatically. To increase the accuracy of the measured data the system acquires 50 data items for every position of the five-hole probe with the sampling frequency of 10 Hz.



Fig. 6. Pneumatic five-holes probe

## 6 Measured and calculated quantities

The main measured quantity detected by the pneumatic probe is the main velocity vector and its components to the axes of the Cartesian system. The orientation of the Cartesian coordinate system is defined by the direction of the central hole orifice axis for the x-axis of the system with the same orientation as the flow direction, y-axis is horizontally oriented and z-axis is vertically oriented in the plane orthogonal to the x axis. As the kinematic system of the traversing device is cylindrical with the coordinates  $x, \varphi, r$ , it is necessary to transform the measured data in every measuring position to the fixed Cartesian system of the measuring planes of the tested model. These transformations of the measured velocity vector angles are performed by a special program directly in the course of measurements. The values and angles of the mean velocity vector are calculated by means of measured individual aerodynamic and directional characteristics of the used probe. From the defined position of the probe and measured pressures in five orifices of the probe and the total temperature of the flow, the static and total pressures of the flow and two angles defining the direction of the velocity vector are calculated.

### 6.1 Measured quantities

Static pressure	$p_s$
Total pressure	$p_t$
Dynamic pressure	$p_d$
Flow quantity	$Q$
Cartesian components of the mean velocity vector	$w_x$ $w_y$ $w_z$

### 6.2 Calculated quantities

To evaluate the value of the generated curl of the velocity of the flow field with respect to the inlet flow conditions, the streamwise component of the vorticity vector of the mean velocity field in the measured planes is calculated using the following equation:

$$\omega_x = \frac{\partial w_z}{\partial y} - \frac{\partial w_y}{\partial z} \quad (1)$$

To evaluate the value of the dissipation of energy by friction and mixing within the curved tube, the local internal loss coefficient is calculated by the following definition:

$$\zeta_l = \frac{p_t - p_{tref}}{p_{dref}} \quad (2)$$

$p_{tref}$  is an upstream reference mean total pressure defined by the expression:

$$p_{tref} = \frac{\iint_A (p_s + \frac{1}{2} \cdot \rho \cdot w^2) \cdot \rho \cdot w_x \cdot dA}{\iint_A \rho \cdot w_x \cdot dA} \quad (3)$$

$p_{dref}$  is an upstream reference mean dynamic pressure defined by the expression:

$$p_{dref} = \frac{\iint_A \frac{1}{2} \cdot \rho \cdot w^3 \cdot dA}{\iint_A \rho \cdot w_x \cdot dA} \quad (4)$$

The mean value of the total pressure at the outlet section C is then:

$$p_t = \frac{\iint_C (p_s + \frac{1}{2} \cdot w^2) \cdot \rho \cdot w_x \cdot dC}{\iint_C \rho \cdot w_x \cdot dC} \quad (5)$$

The internal integral loss coefficient of the flow within the whole curved tube including the outlet pipe is given by the integration of the local internal loss coefficient over the outlet section C.

The integral value of the internal loss coefficient of the curved tube is then given by the expression:

$$\zeta = \frac{p_t - p_{tref}}{p_{dref}} \quad (6)$$

In reality the transversal component of the kinetic energy of the flow at the outlet section C of the curved tube which is mainly created by

the secondary flow vortexes is non-recuperative and it is later gradually dissipated by the friction. The real loss of energy is then given as a sum of the energy loss caused by dissipation in the curved tube produced by the friction and mixing and by the kinetic energy  $e_u$  of the transversal component of the motion of the air within the plane  $y$ - $z$ .

Local dynamic pressure corresponding to this transversal component of the kinetic energy is then:

$$p_{ldu} = \frac{1}{2} \cdot \rho \cdot (w_y^2 + w_z^2) \quad (7)$$

The local loss coefficient corresponding to the kinetic energy of the transversal component of the flow is then given by:

$$\zeta_{kinu} = \frac{p_{ldu}}{p_{dref}} \quad (8)$$

The total local internal loss coefficient

$$\zeta_{tot} = \zeta_l + \zeta_{kinu} \quad (9)$$

The integral value of the dynamic pressure corresponding to the transversal velocity component is given by the expression:

$$p_{du} = \frac{\iint \frac{1}{2} \cdot (w_y^2 + w_z^2) \cdot w_x \cdot \rho \cdot dC}{\iint_A \rho \cdot w_x \cdot dA} \quad (10)$$

The value of the integral loss coefficient of the transversal kinetic energy component is then:

$$\zeta_{kinu} = \frac{p_{du}}{p_{dref}} \quad (11)$$

The total integral loss coefficient of the curved tube is then given by the sum of the integral internal loss coefficient and integral loss coefficient corresponding to the transversal component of kinetic energy.

$$\zeta_{tot} = \zeta + \zeta_{kinu} \quad (12)$$

## 7 Measurements

The measurements have been performed at the aerodynamic laboratory of the Department of Fluid Dynamics and Thermodynamics of the Faculty of Mechanical Engineering of the Czech Technical University in Prague [5] using the described low turbulence wind tunnel.

Two different cases of the inflow structure and turbulence at the inlet section of the tested aerodynamic model have been examined.

The first case marked as Case 1 was realized by connecting of the tested model directly to the outlet section of the accelerating nozzle of the wind tunnel as shown in Fig. 7. In this case the inlet flow to the tested model is very homogenous with a very uniform measured velocity distribution (see Fig. 5). The intensity of turbulence of the flow and its distribution measured by a hot wire probe was also low with maximum value of 0.25% at the used mean velocity of 40 m/s. The mass flow of the air at the atmospheric conditions has been maintained constant during the measurements. For every adjusted and controlled to the same value.

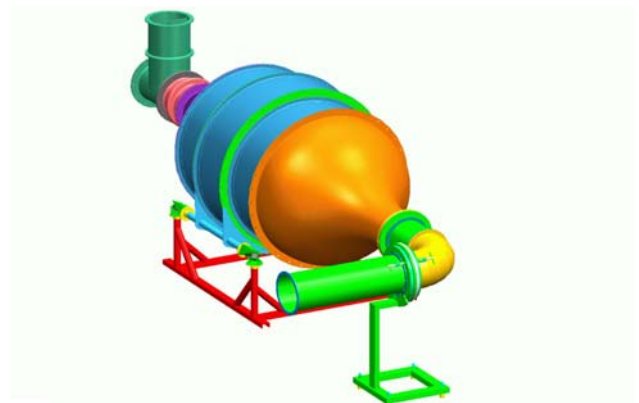


Fig. 7. Configuration of the experiment – Case 1

The second case marked as Case 2 was realized by inserting a smooth straight circular pipe of a length of 18 meters between the accelerating nozzle of the wind tunnel and the tested model. In this case the inlet flow conditions at the tested model correspond to the fully developed turbulent pipe flow of the standard characteristics that are assured by the straight, smooth circular pipe of the length of 60

diameters. The mean velocity distribution as well as the turbulence characteristics have been measured and verified by the hot wire probe with oblique oriented wire. The configuration of the measurements in Case 2 is shown in Fig. 8. The experiments have been performed at the same mass flow as those in Case 1.

Mean velocity distributions in three measuring planes A, B and C were measured at the tested model. The experiments were performed for the same mass flow  $Q$  and the same Reynolds and Dean numbers with two different inlet flow structure conditions noted as Case 1 for a homogenous low turbulence inflow and as Case 2 for a fully developed turbulent velocity profile. The mean velocity vectors were measured using a micro-pneumatic five-hole probe. The flow fields were traversed in 1369 points and in every point five pressure values were sampled for 5 second with a sampling frequency of 10 Hz. The acquired data were stored in the computer and then evaluated.

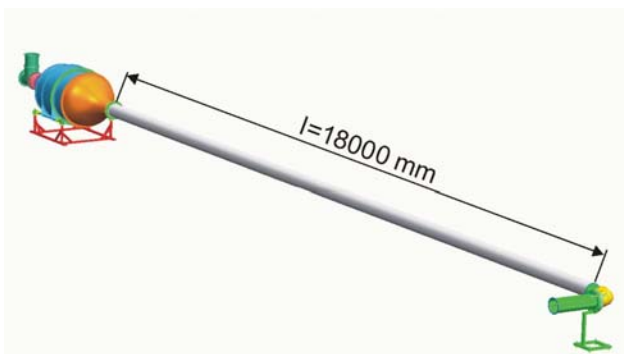


Fig. 8. Configuration of the experiment – Case 2

### 7.1 Results of the measurements

For the inlet flow conditions as described above the Reynolds and Dean numbers of the experiments were:

$$M = 0.12$$
$$Re = 818000$$
$$De = 808000$$

The results of the measurements are presented in the form of clearly organized diagrams shown in Figures 9-13. In the figures the measured and calculated variables are clearly presented

starting with the inlet measuring plane A through the intermediate measuring plane B to the outlet plane C in such a way that Case 1 and Case 2 are presented side by side to make comparing easy.

### 7.2 Accuracy of the measurements

Based on the number of measurements carried out repeatedly on the calibrating track, reproducibility of measurements and decisive deviation from the mean obtained values were evaluated. As far as established deviations are concerned, the measured velocities are determined with a precision of the velocity module error smaller than 1%, and the angles with an error in the precision of determining the direction of the time mean vector of velocity in the area of the total range of angles of attack of the flow measured in relation to the axis of the central hole of the probe, which is  $\pm 27$  degrees. An error smaller than 0.5 degree was found in this range of measurements.

To guarantee measurement precision the pneumatic probe was calibrated twice for each measuring case. The first calibration was carried out prior to and the second after the measurement. Based on the comparison of two pairs of the measurements the verification of the time stability of aerodynamic characteristics of the probe proved very satisfactory reproducibility of measurements with the maximum deviations of measured modules of the mean velocity vectors and their direction of the order of used measuring method errors. Checks carried out confirmed that in the course of measurements no greater change in the characteristics of the probe occurred.

### 7.3 Discussion

The first stage of the measurements of turbulent 3-D mean flow fields in the tested model of a curved duct enables to preliminary quantify the influence of two tested inlet flow structures on the formation of secondary flow and in particular on the process of the forming of the two counter-rotating vortices which create the well-known horse-shoe vortex

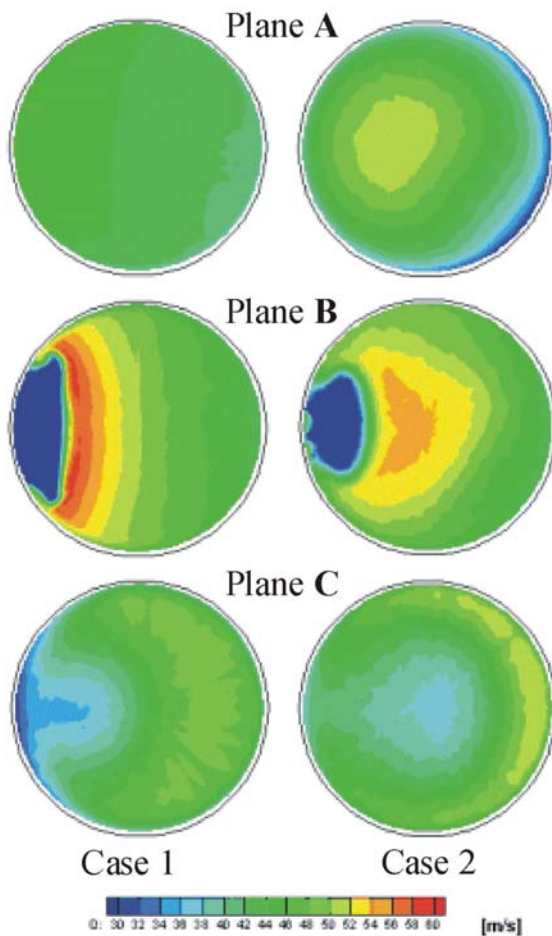


Fig. 9. Module of the mean velocity  $w$  distribution

in the form of two vortex tubes connected and anchored in the elbow with their open ends flowing away with the flow from the curved duct. According to the theoretical assumptions the area of secondary flow at the outlet section C and the intensity of the vortices are tied with the boundary layers thickness on the walls in the inlet and curved part of the tube. In Case 1 this area is very small, also the size of vortices is very small, thus they dissipate before they reach the measuring C plane (see Fig. 13).

But on the other hand, in the case where the in-coming flow has a boundary layer fully penetrating as far as the tube axis, a significant secondary flow with flowing away vortices is formed where the vortices are indicated in the measuring C plane.

As to the image of the flow in the elbow, the measurement carried out

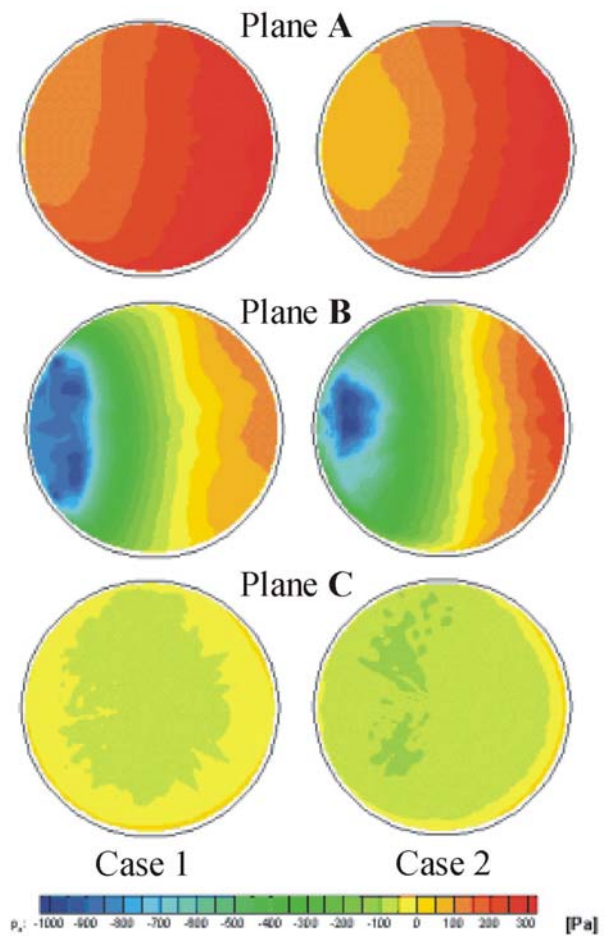


Fig.10. Static pressure  $p_s$  distribution

so far has made only information on velocity and pressure fields in the plane B located directly after the elbow bend available. In both studied cases the areas of flow separation in the suction side of the wall are indicated, the measured separation areas in both cases differ in size and shape. In Case 1 the separation area is larger and wider while in Case 2 its shape is more compact. As to the C cross-section directly before the outlet into atmosphere, the flow in both cases flows out from a full cross-section; in Case 1 at the measuring plane C it is clear that the area with a highest loss is adjacent directly to the suction side of the wall while in Case 2 it is located in the center of the tube. The measured value of the internal loss coefficient is worthy of attention. In the case of turbulent flow this coefficient is only slightly higher than in the case of laminar inflow.

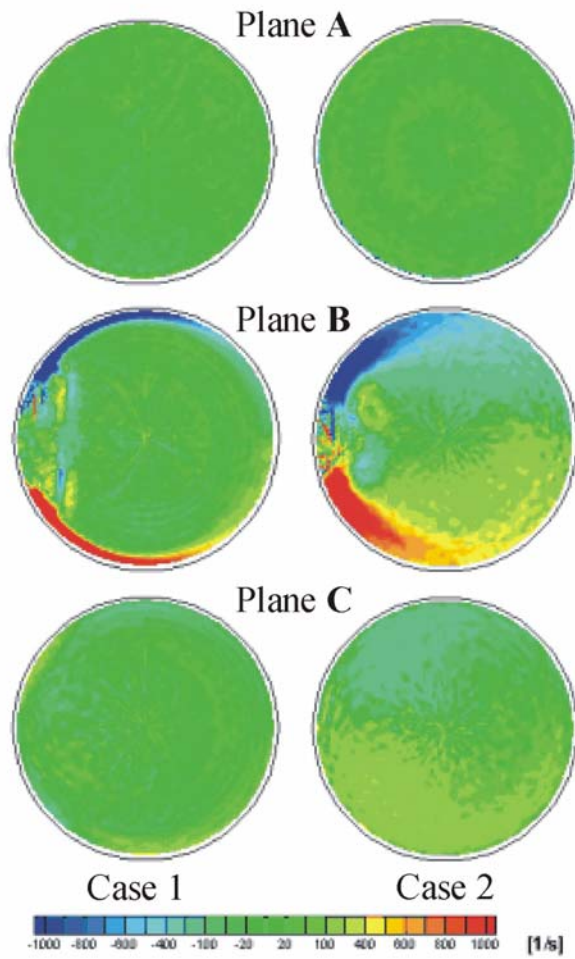


Fig. 11. Streamwise vorticity component  $\omega_x$  distribution

This measured loss coefficient representing energy dissipation caused by friction and mixing shows that the cumulative influence of both dissipation mechanisms in both measured cases does not differ significantly. From this we can conclude that the increased friction losses in the turbulent flow case are compensated for by smaller mixing losses due to a smaller area of separation.

If the loss due to the transversal component of the out-flowing kinetic energy is added to the internal loss in the elbow, we obtain a total loss coefficient that, in the case of turbulent flow, represents an absolute increase of 1 % in the loss coefficient.

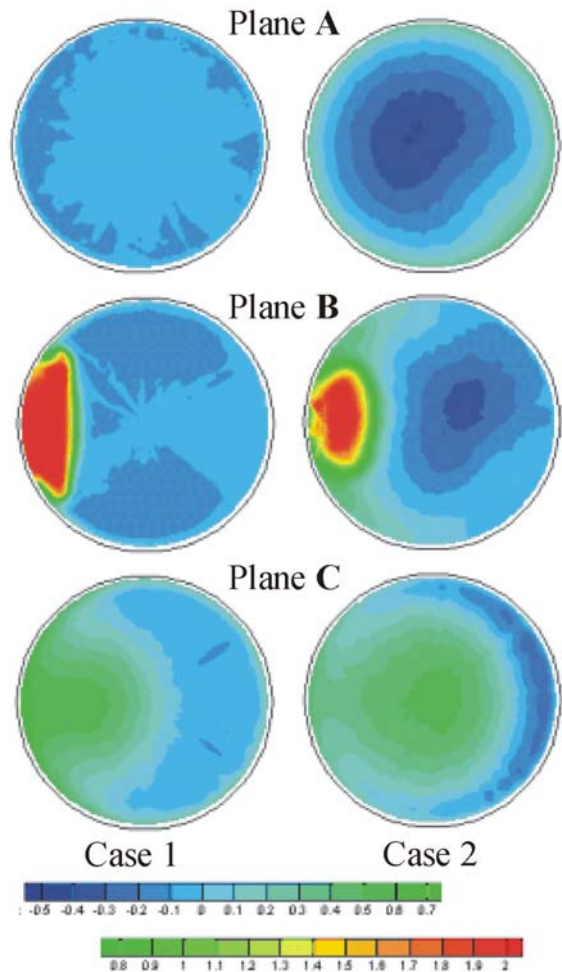


Fig. 12. Total internal loss coefficient  $\zeta_{tot}$  distribution

**Measured values of the loss coefficients:**

Loss coefficient	$\zeta$	$\zeta_{skinu}$	$\zeta_{tot}$
Case 1	0.235	0.0003	0.235
Case 2	0.273	0.0090	0.282

**8 Conclusion**

The first stage of our carried-out measurement proves the influence of the inlet flow structure and turbulence on the total flow field in the elbow and on the development of a secondary flow which is characterized by the formation of two counter-rotating flowing away vortices. While in the case of a homogenous inlet velocity field with low turbulence intensity the whirling movement was not indicated in the

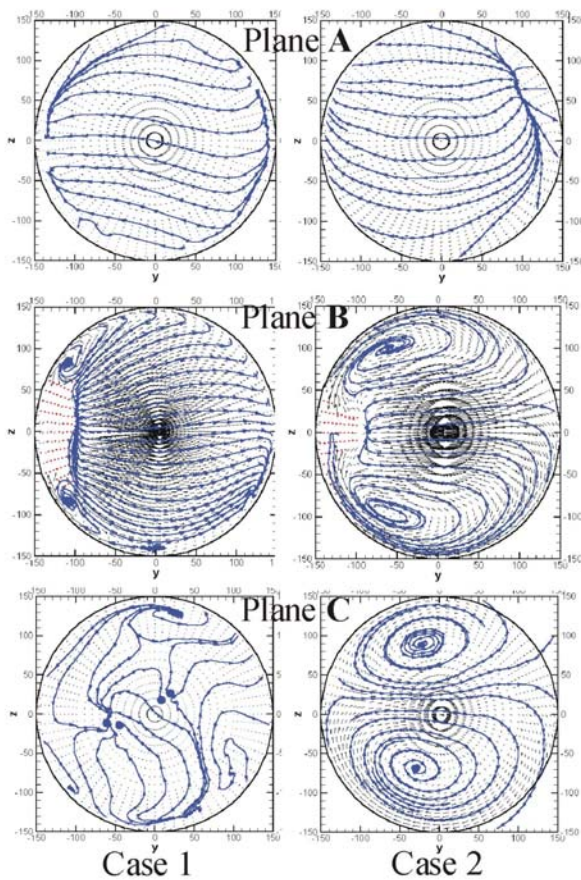


Fig. 13. Transversal velocity  $\vec{w}_u = \vec{w}_y + \vec{w}_z$  distribution

outlet cross-section of the measured model, in the case with the fully developed inlet turbulent velocity profile the whirling movement was considerable though of comparatively smaller importance from the energy point of view. Experimental research work on 3-D turbulent flow in the field of internal aerodynamics represented in the above-mentioned example aims at examining the phenomena from a physical point of view as well as preparation of experimental data for testing both commercial and in-house CFD methods. That is why measurements of time-dependent flow velocity vector are planned with the use of a thermo-anemometric method with a triaxial hot wire or film probe including visualisation experiments and measurement of flow fields by means of Particle Image Velocimetry.

## 9 Acknowledgements

This research was carried out in the Aerospace Research Center supported by the Czech Ministry of Education, Sports and Youth, by grant No LN 00B 051 and as a part of the project supported by grant No J04/98:212 2 00009.

## 10 References

- [1] Jerie J. Elementare Theorie der Doppelwirbel in gekrümmten Kanälen. *Wissenschaftliche Zeitschrift der Technischen Universität Dresden*, Vol. 37, Heft 6, 1988.
- [2] Hanus D. Inlet and Outlet Casings of the Turbojet Engine – Design and Experiment. *Acta Polytechnica – Journal of Advanced Engineering Design*, CTU in Prague, Vol. 40, No. 4/2000, pp 101-110, 2000.
- [3] Censky T, Hanus D. Aerodynamical Design of the Low Turbulence Tunnel by CFD Methods. *Proceedings of the International Conference on Advanced Engineering Design*, University of Glasgow, pp. 87-92, 2001.
- [4] Anderle P, Hanus, D. Design of Low Turbulence Wind Tunnel for Investigation of Three-Dimensional Unsteady Flow. *Proceedings of the International Conference on Advanced Engineering Design*, University of Glasgow, pp. 93-98, 2001
- [5] Uruba V, Jonas P, Mazur O, Hanus D. Measurements of the Flow fields within the Elbow of Circular Cross Section (In Czech). *Proceedings of the 13 th International Conference on Application of Experimental and Computational Methods in Fluid Dynamics*, University of Zilina, Slovak Republic, Zilina, pp. 12-17, 2002.